PROCEEDINGS OF SPIE

SPIEDigitalLibrary.org/conference-proceedings-of-spie

Real-time quantification of salicylic acid with a fiber optic sensor functionalized by gold nanoparticles-copper metal organic conjugate coating

Shawana Tabassum

Shawana Tabassum, "Real-time quantification of salicylic acid with a fiber optic sensor functionalized by gold nanoparticles-copper metal organic conjugate coating," Proc. SPIE 12120, Sensing for Agriculture and Food Quality and Safety XIV, 1212009 (1 June 2022); doi: 10.1117/12.2605711

SPIE.

Event: SPIE Defense + Commercial Sensing, 2022, Orlando, Florida, United States

Downloaded From: https://www.spiedigitallibrary.org/conference-proceedings-of-spie on 03 Feb 2023 Terms of Use: https://www.spiedigitallibrary.org/terms-of-use

Real-time Quantification of Salicylic Acid with a Fiber Optic Sensor Functionalized by Gold Nanoparticles-Copper Metal Organic Conjugate Coating

Shawana Tabassum[a]*
[a]Electrical Engineering, the University of Texas at Tyler, Tyler, TX, USA
*Corresponding author: stabassum@uttyler.edu

ABSTRACT

Salicylic acid (SA) is a vital regulator of induced defense mechanisms in plants. Progressive variations in the SA levels have been reported in many droughts, salt, and cold/heat-stressed plants, as well as after pathogen/herbivore attacks. Hence, real-time and *in situ* monitoring of this phytohormone will facilitate the early identification of crop stresses so that immediate interventions can be implemented to mitigate productivity losses and maintain the quality of the product (e.g., quality of produce and cotton fibers). However, the lack of *in situ* and localized analysis capabilities in current technologies limits their use in crop fields. Toward this endeavor, this work reports an LSPR (localized surface plasmon resonance)-based fiber-optic sensor functionalized with a conjugate of gold nanoparticles and copper-based metal-organic framework (CuMOF) for selectively measuring SA levels in sap. For this purpose, the distal end of an optical fiber was coated with gold nanoparticles that exhibited LSPR upon excitation by light's electromagnetic field. The gold nanoparticles-coated fiber was covalently functionalized with CuMOF, which selectively oxidized SA. This oxidation reaction resulted in a variation in the local refractive index, thereby leading to a change in the LSPR intensity level. The fiber-tip sensor exhibited a sensitivity of up to 0.0117 % light reflection variations per μM concentration of SA and a limit of detection of 37 μM. Plant sap was used to calibrate the sensor for precision measurements. The fiber-tip sensor was also demonstrated to measure the SA levels in the stem of a live plant. Considering excellent dynamic detection range (100-1000 μM) and sensitive thiol chemistry, the developed sensor could hold promises in future *in situ* probe development for real-time measurements of phytohormones in sap.

Keywords: Fiber-optic sensor, salicylic acid, precision farming, water stress, copper metal-organic nanocomposite, gold nanoparticles, localized surface plasmon resonance.

1. INTRODUCTION

Environmental stresses induce a progressive change in the levels of phytohormones circulating in the xylem and phloem of plants. These phytohormones serve as early signals of plant stress. Salicylic acid (SA), Jasmonic acid (JA), Abscisic acid (ABA), Indole-3-acetic acid (IAA), and volatile organic compounds such as ethylene (ET) are among the most important regulators of induced defense mechanisms [1-7]. Progressive variations in their levels have been reported under drought, salt, and cold/heat-stressed conditions [8-10]. However, the dynamic interaction mechanism of these hormones is not fully elucidated under environmental stress conditions due to the lack of technology needed to facilitate *in situ* sensing. Our central hypothesis is that real-time data on plant hormone levels can be used to determine the fundamental ways plants interact with and adapt to the stressors.

The high-performance liquid chromatography (HPLC) and nuclear magnetic resonance (NMR) imager are the traditional, quantitative precision methods, which require tissue samples to be extracted and taken to a laboratory. Although these methods provide metabolite profiling, high repeatability, and testing accuracy due to controlled conditions in the laboratory, they incur destructive sample collection from the plants. Moreover, the collected samples lose their functionality due to the need to transport long distances to the lab. The time lag between sample collection and analysis prevents follow-up and dynamic studies [11]. Due to the complexities and time delays associated with these techniques, only a few plants are sampled, and extrapolations are made about the whole population, thereby neglecting the significant variations between plants across a field. Infrared spectrometer and thermal imager are the imaging techniques that provide a non-disruptive view of the action of the stressors in plants. However, these approaches lack accuracy and wireless communication protocol, do not provide quantitative analysis of metabolites, and are effective only at late crop responses

Sensing for Agriculture and Food Quality and Safety XIV, edited by Moon S. Kim,
Byoung-Kwan Cho, Proc. of SPIE Vol. 12120, 1212009
© 2022 SPIE · 0277-786X · doi: 10.1117/12.2605711

Downloaded From: https://www.spiedigitallibrary.org/conference-proceedings-of-spie on 03 Feb 2023
Terms of Use: https://www.spiedigitallibrary.org/terms-of-use

[11]. Unmanned aerial systems (UAS) have emerged as an attractive tool for aerial scouting. They can fly to waypoints, hover, and collect high-resolution data (millimeters per pixel) from large acres of the field quickly. However, UASs only collect phenotype data (e.g., chlorophyll and vegetation index, plant counting, elevation and volume, organ counting, disease detection) by periodically capturing crop images with a spectral camera and not conducting chemical profiling. Moreover, UASs are very power-hungry and frequently require human intervention for battery recharge/replacement. It can take an entire 8-hours workday to exhaustively collect high-definition images from every zone in an 80-acre crop field [12-14]. FloraPulse and Dynamax are commercial devices that have emerged as *in situ* plant monitoring tools [15, 16]. However, the FloraPulse and Dynamax sensors only monitor sap water content and do not provide chemical (e.g., metabolite or nutrient) profiling. None of these commercial crop sensors can provide real-time and continuous monitoring of stress responses in plants. In contrast, repeated *in situ* measurements of metabolites can provide valuable information about the onset and dynamics of stress responses in plants.

Toward this endeavor, this paper reports an optical fiber-based sensor for quantitatively monitoring the salicylic acid (SA) levels in live plants. The tip of an optical fiber was coated with a complex conjugate of gold nanoparticles and a copper-based metal-organic framework (CuMOF). Gold nanoparticles generated localized surface plasmon resonance (LSPR), and CuMOF provided selective oxidation of SA on the sensor surface. The micron-scale fiber-tip sensor was inserted inside the stem of a live plant to measure the SA levels *in situ* and in real-time. Our proposed sensor overcomes the mentioned limitations by providing continuous and *in situ* monitoring capabilities while incurring minimal damage to the plant. In addition, the fiber-optic sensor advances our earlier work on a leaf-mounted SA sensor by eliminating the need for manual sap collection [17].

2. MATERIALS AND METHODS

2.1 Reagents

Hydrogen tetrachloroaurate (III) hydrate ($HAuCl_4$), trisodium citrate, sulfuric acid (H_2SO_4), hydrogen peroxide (H_2O_2), 3-mercaptopropyltriethoxysilane (MPTES), methanol, acetic acid, 4-aminobenzenethiol, N, N-dimethylformamide (DMF), polyvinyl pyrrolidone (PVP), copper (II) nitrate, 2-amino terephthalic acid, and salicylic acid (SA) were obtained from Sigma Aldrich (St. Louis, MO).

2.2 Experimental Setup

Optical measurements were carried out using a fiber-coupled light source (Thorlabs, Newton, NJ) and a UV-Vis spectrometer (Ocean Insight, Orlando, FL). One end of a 2 × 1 multimode fiber coupler (Thorlabs) was connected to the light source, and the other end was connected to the spectrometer (Figure 1a). The SA sensor was fabricated on the fused tip of the fiber, which was inserted inside the stem through a punched hole (Figure 1b-c). The evanescent field of the light guided through the fiber core interacted with the sensing layer at the distal end and excited localized surface plasmon resonance (LSPR). At LSPR, the reflected light had minimum intensity.

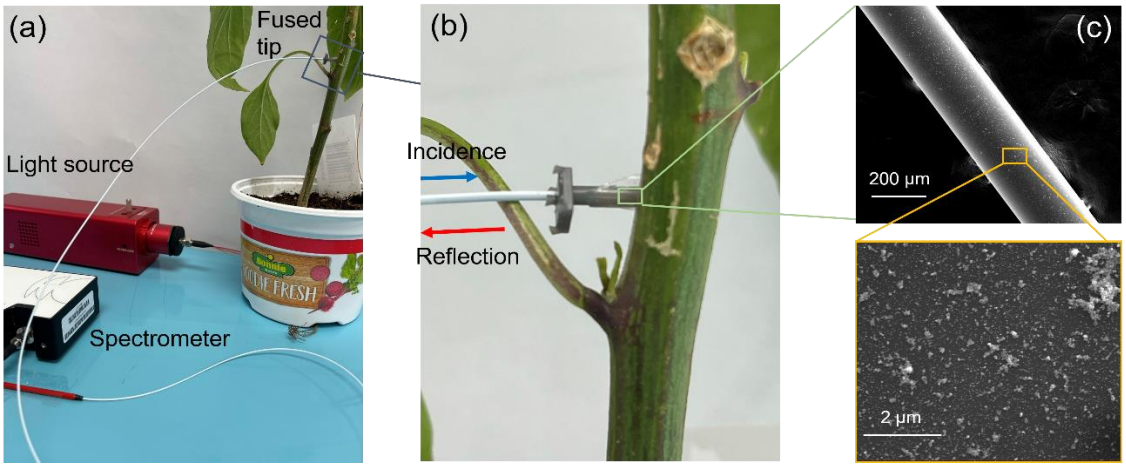

Figure 1: (a) Optical setup for SA measurements with the fiber-tip sensor. Inset in (b) shows the *in situ* SA measurements in the stem of a live plant. Inset in (c) shows the scanning electron microscopic images of the fiber-tip sensor.

Downloaded From: https://www.spiedigitallibrary.org/conference-proceedings-of-spie on 03 Feb 2023
Terms of Use: https://www.spiedigitallibrary.org/terms-of-use

3. DEVICE FABRICATION AND CHARACTERIZATION

3.1 Functionalizing the Optical Fiber with Gold Nanoparticles (AuNPs)-CuMOF Conjugate

The AuNPs solution was prepared by the Turkevich method, as explained in [18]. The CuMOF solution was prepared using the procedure outlined in [17].

To functionalize the distal end of a fused fiber with AuNPs, the silica fiber was first de-cladded using acetone. The unclad area of the fiber was next hydrolyzed with Piranha solution (volume ratio of H_2SO_4:H_2O_2 = 7:3) for 30 min at 85^{0}C, which provided –OH groups on the fiber surface. Following that, the optical fiber was rinsed with DI water, blow-dried with N_2, and annealed in a vacuum oven for 30 min at 110^{0}C.

Afterward, a sol-gel deposition process was used to functionalize thiol groups on the fiber surface. This procedure started with the formation of an aqueous/alcohol solution (75% distilled water:25% methanol, pH = 4.5±0.2 with acetic acid) [12]. Then MPTES was added to yield a 2% (v/v) final concentration, allowing 10 min for the hydrolysis of alkoxide and silanol formation. The fiber was immersed in this solution for 30 min and then rinsed with ethanol to remove unbound silane from the surface. The fiber was then annealed at 110^{0}C for 30 min for condensation reactions, which provided -SH groups on the surface.

Finally, 1 ml of 0.2 mg mL^{-1} 4-aminobenzenethiol solution and 0.1 mL of as-prepared CuMOF solution were added to 0.9 ml of phosphate buffered saline (pH 6.0). The reaction proceeded at room temperature for 5 min. Next, 1 ml of AuNPs suspension was added, and the mixture was incubated for 15 min. After the incubation, the silane-coated fiber was dipped into the resulting solution for 12 hours. Figure 2 illustrates the step-by-step functionalizing procedure.

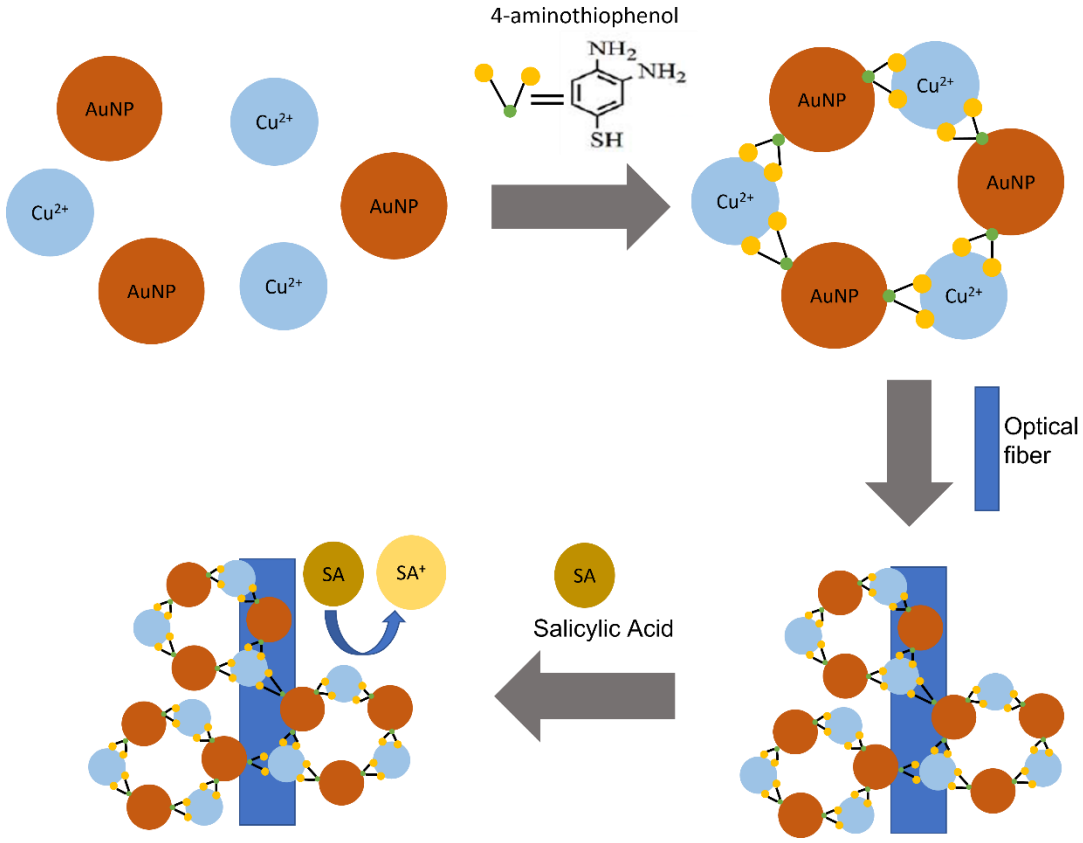

Figure 2: Step-by-step process flow for functionalizing the optical fiber with AuNPs-CuMOF conjugate coating that selectively oxidizes SA.

Downloaded From: https://www.spiedigitallibrary.org/conference-proceedings-of-spie on 03 Feb 2023
Terms of Use: https://www.spiedigitallibrary.org/terms-of-use

3.2 Characterization

Figure 3a shows the scanning electron microscopic (SEM) images of the AuNPs-CuMOF coated optical fiber for different magnifications. The uniform morphology of the composite coating on the cylindrical fiber surface is evident from the SEM images. The UV-Vis spectroscopy in Figure 3b demonstrates the absorption peaks for AuNPs alone and then for the AuNP-CuMOF composite coating. The AuNPs have an absorption peak at 542 nm, whereas the composite layer has three distinct absorption peaks. The AuNPs peak is shifted to 564 nm in the composite. The two remaining peaks at approximately 676 nm and 730 nm can be attributed to the light absorption by the AuNP-Cu^{2+} conjugate. The findings from the UV-Vis spectroscopy was later confirmed from the reflection spectra of the fiber-tip sensor, as is explained in Section 4.1 (Figure 4a). The CuMOF coating was further characterized with Fourier Transform Infrared Spectroscopy (FTIR), as is demonstrated in Figure 3c. The FTIR spectrum confirmed the presence of amino groups and -OH and C=O functional groups, also reported in the literature [19].

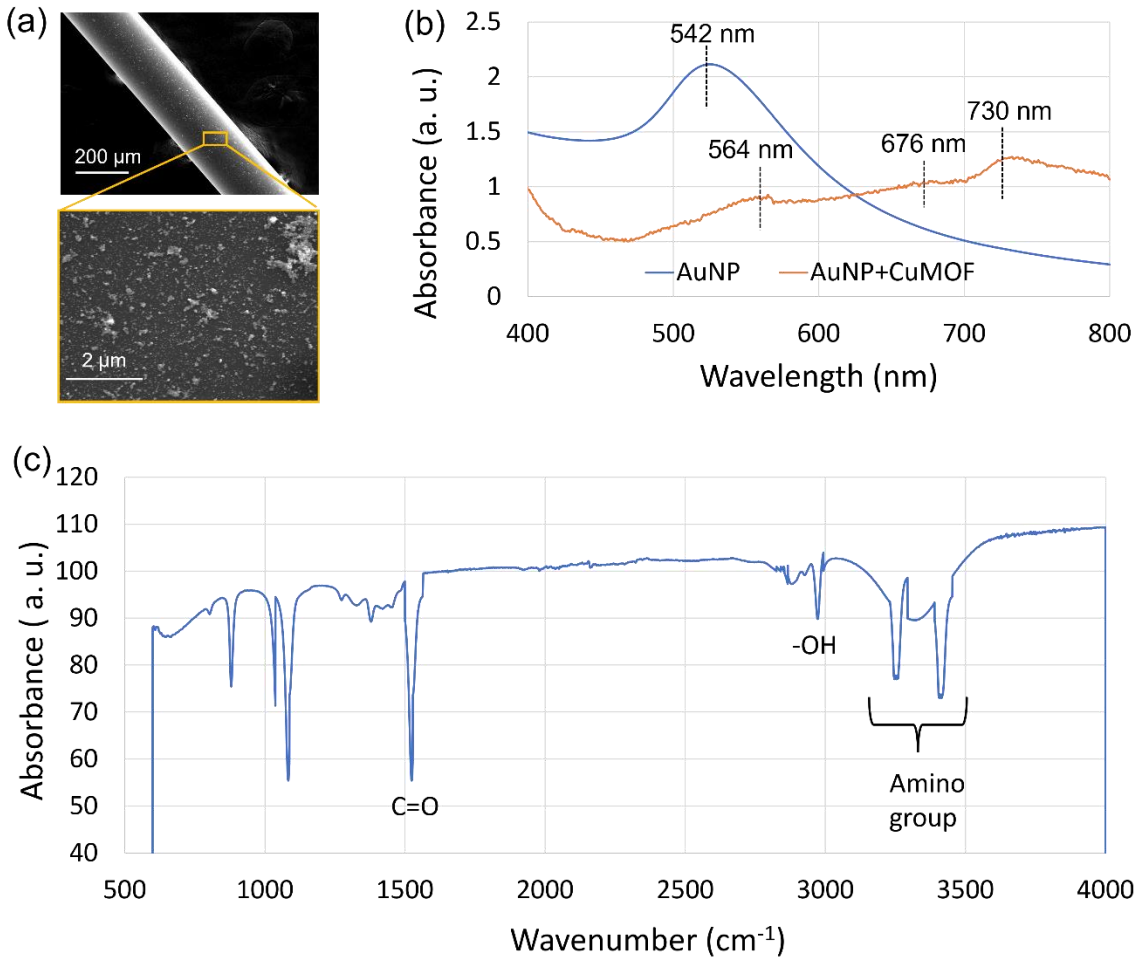

Figure 3: (a) Scanning electron microscopic (SEM) images of the AuNPs coated fiber-tip sensor at 150x (top panel) and 20000x (bottom panel) magnifications. (b) UV-Vis spectroscopy of AuNPs and AuNPs-CuMOF conjugate. (c) Fourier Transform Infrared Spectroscopy (FTIR) of the CuMOF coating.

Downloaded From: https://www.spiedigitallibrary.org/conference-proceedings-of-spie on 03 Feb 2023
Terms of Use: https://www.spiedigitallibrary.org/terms-of-use

4. RESULTS AND DISCUSSION

4.1 LSPR Sensing of SA

The sensor was calibrated with plant sap extracted from the stem of cabbage plants using standard extraction tools. The extracted sap was centrifuged at 1000 rpm for 1 hour to precipitate the debris and other solid compounds. The supernatant was collected and stored at -1°C for future use.

Figure 4a shows the reflection spectra for five SA concentrations ranging from 100 to 1000 µM spiked in the plant sap. This range includes the SA concentrations typically found in unstressed and stressed bell pepper, tomato, and cabbage plants. The phytohormone levels in unstressed plants range from 50-200 µM [20-27]. With increasing SA concentrations, the LSPR intensity increased due to the oxidation of SA molecules and hence an increase in the refractive index at the sensor surface. The sensor reflection spectra had distinct LSPR dips at 542, 676, and 730 nm, which were also observed from UV-Vis spectroscopy (Figure 3b). Calibration curves were generated by plotting LSPR intensity variations with respect to the baseline (i.e., 0 µM of SA) vs. SA concentrations at 542 and 730 nm (Figure 4b-c). The sensitivity and limit of detection at 542 nm were found to be 0.0117 μM^{-1} and 50.5 µM, respectively. The sensitivity and limit of detection at 730 nm were found to be 0.0115 μM^{-1} and 37.6 µM, respectively.

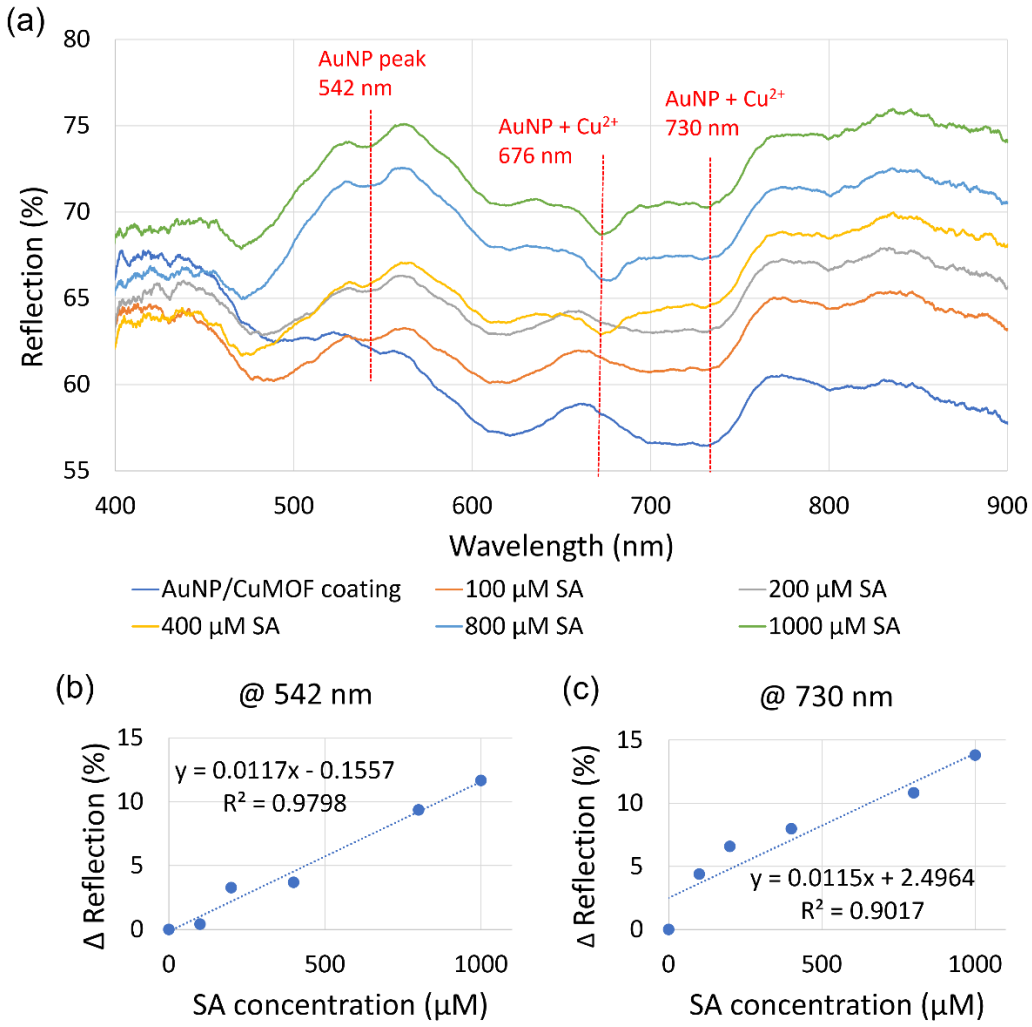

Figure 4: (a) Reflection spectra of the AuNPs-CuMOF coated fiber-tip sensor for different concentrations of SA oxidized at the sensor surface. Calibration plot of LSPR intensity changes versus SA concentrations at (b) 542 nm and (c) 730 nm.

Downloaded From: https://www.spiedigitallibrary.org/conference-proceedings-of-spie on 03 Feb 2023
Terms of Use: https://www.spiedigitallibrary.org/terms-of-use

To verify that the shifts in the LSPR spectra were due to the selective oxidation of SA by the CuMOF coating, we used a bare de-cladded optical fiber as the control. The control fiber was tested with the same SA concentrations. No noticeable shifts in the reflection spectra were observed with the control fiber (Figure 5) compared to the sensor fiber (Figure 4).

4.2 Real-time SA Measurements in Live Plants

Figure 6a shows the dynamic variations in the reflection spectra when the fiber-tip sensor was inserted in the stem of a live cabbage plant through a 1 mm diameter hole. The hole was carefully punched to cause a minimal insertion damage to the

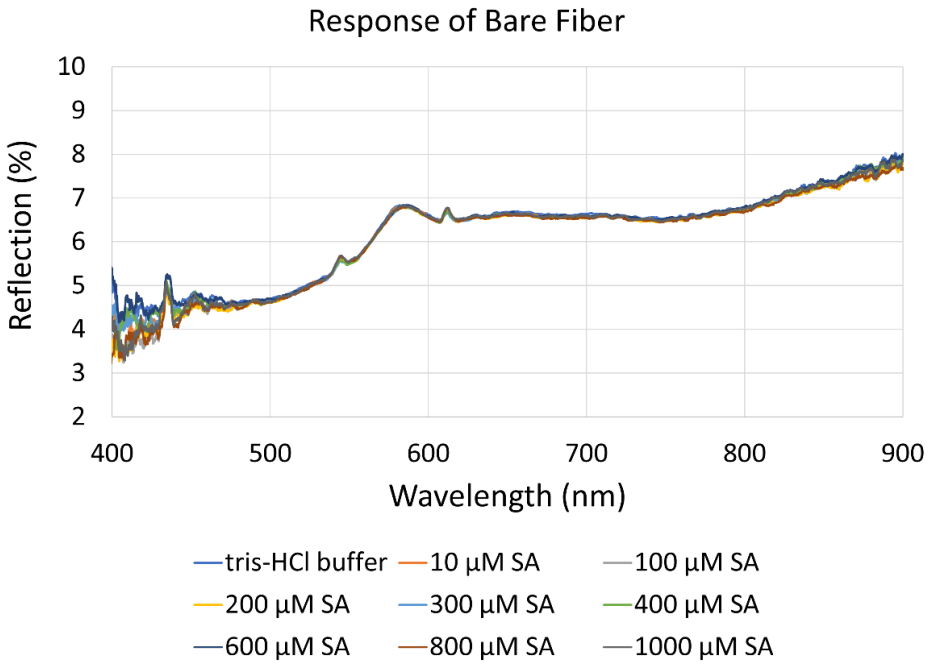

Figure 5: Reflection spectra of the bare fiber for different concentrations of SA.

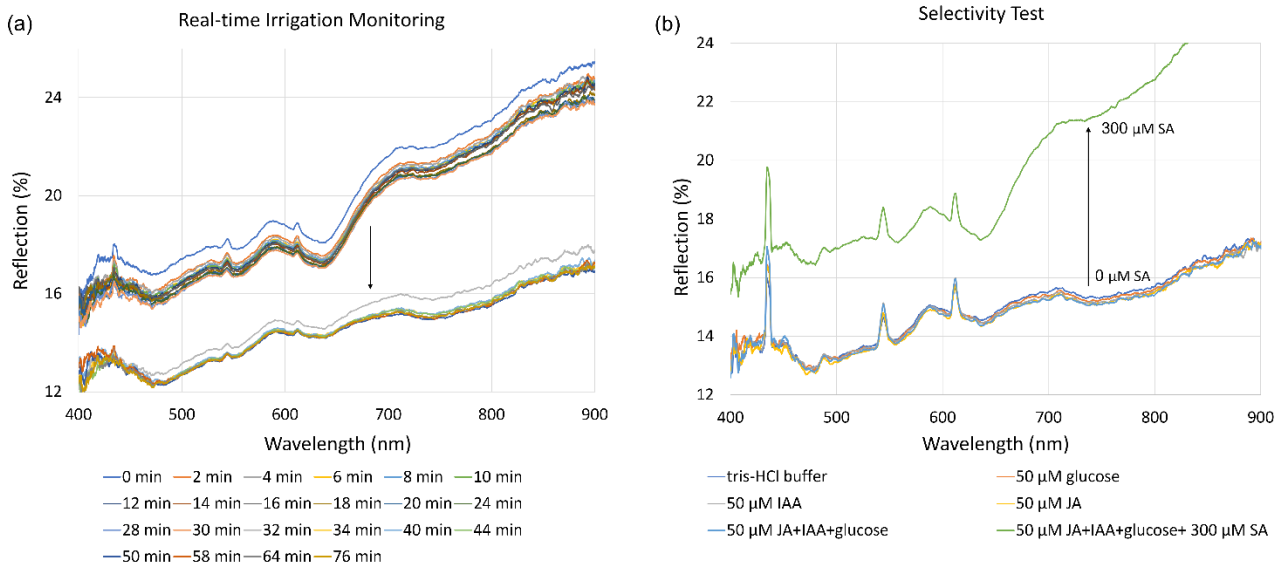

Figure 6: (a) Real-time reflection spectra measured over 76 minutes. (b) Reflection spectra for different interfering species introduced to the fiber-tip sensor.

Downloaded From: https://www.spiedigitallibrary.org/conference-proceedings-of-spie on 03 Feb 2023
Terms of Use: https://www.spiedigitallibrary.org/terms-of-use

plant. Before taking the measurements, the plant was under water stress for three days. Next, the plant was irrigated, and the measurements were recorded over 76 min. It was observed that the reflection intensity reduced after 32 min (as denoted by the downward arrow in Figure 6a). This could be attributed to the reduction in the SA level, as was confirmed through the calibration plots in Figure 4b-c. Irrigation resulted in water stress mitigation and, hence, a reduced SA level was measured with the sensor. In addition, the sensor could accurately estimate the SA concentrations during the 76 min period, as was confirmed by high-performance liquid chromatography tests, suggesting the reliability of the sensor. The water-stressed plant had an initial SA concentration of 72 μM and after irrigation the SA level reduced to 66 μM.

4.3 Selectivity Test

The sensor was tested against different interfering species commonly found in the plant sap. The following solutions were used for the selectivity test: (i) 50 μM glucose, (ii) 50 μM Indole-3-acetic acid (IAA), (iii) 50 μM Jasmonic acid (JA), (iv) a mixture of 50 μM JA, 50 μM IAA, and 50 μM glucose, and (v) a mixture of 50 μM JA, 50 μM IAA, 50 μM glucose, and 300 μM SA. It was evident that the sensor response did not demonstrate any noticeable variations in the absence of SA. When SA was added to the mixture, a significant shift in the reflection spectrum was observed. The measured spectra are demonstrated in Figure 6b. The amount of intensity shift at the resonance wavelength of ~730 nm was commensurate with the calibration curve in Figure 4c for 300 μM of SA.

5. CONCLUSION

This work reports an LSPR sensor manufactured at the tip of an optical fiber and coated with CuMOF for selective monitoring of a key defense-related phytohormone, salicylic acid (SA). The sensor demonstrated a good sensitivity to SA and excellent selectivity against common interfering species found in plant sap. The detection limit was found to be 37.6 μM and a linear detection range up to 1000 μM for SA, which is sufficient for detecting SA levels in stressed and unstressed plants. The fiber-tip sensor was also demonstrated to monitor the SA level changes in the stem of a live cabbage plant, thereby facilitating real-time monitoring of the fundamental ways plants interact with ambient stressors, which is beyond the capability of conventional discrete, disruptive, resource- and time-intensive technologies.

REFERENCES

[1] Spoel, S. H. and Dong, X. “How do plants achieve immunity?: Defense without specialized immune cells,” Nature Reviews Immunology 12:89–100 (2012).

[2] Fu, Z. Q. and Dong, X. “Systemic acquired resistance: Turning local infection into global defense,” Annual Review of Plant Biology 64(1):839–863 (2013).

[3] Vos, I. A., Pieterse, C. M. J., and van Wees, S. C. M. “Costs and benefits of hormone-regulated plant defences,” Plant Pathology 62(S1):43–55 (2013).

[4] Philippot, L., Raaijmakers, J. M., Lemanceau, P., and van der Putten, W. H. “Going back to the roots: the microbial ecology of the rhizosphere,” Nature Reviews Microbiology 11:789–799 (2013).

[5] Mir, M. A., John, R., Alyemeni, M. N., Alam, P., and Ahmad, P. “Jasmonic acid ameliorates alkaline stress by improving growth performance, ascorbate glutathione cycle and glyoxylase system in maize seedlings,” Scientific Reports 8:2831 (2018).

[6] Bari, R. and Jones, J. D. G. “Role of plant hormones in plant defense responses,” Plant Mol. Biol. 69:473–488 (2009).

[7] Kunkel, B. N. and Harper, C. P. “The roles of auxin during interactions between bacterial plant pathogens and their hosts,” J. Experimental Botany 69: 245–254 (2018).

[8] Wang, J., Song, L., Gong, X., Xu, J., and Li, M. “Functions of Jasmonic Acid in plant regulation and response to abiotic stress,” Int. J. Mol. Sci. 21:1446 (2020).

[9] Sah, S. K., Reddy, K. R., and Li, J. “Abscisic acid and abiotic stress tolerance in crop plants,” Frontiers in Plant Sci. 7: 571 (2016).

Downloaded From: https://www.spiedigitallibrary.org/conference-proceedings-of-spie on 03 Feb 2023
Terms of Use: https://www.spiedigitallibrary.org/terms-of-use

[10] Pa´l, M., Janda, T., and Szalai, G. “Abscisic acid may alter the salicylic acid-related abiotic stress response in maize,” J. Agronomy & Crop Science 197: 368–377 (2011).

[11] Galieni, A., Ascenzo, N. D’, Stagnari, F., Pagnani, G., Xie, Q., and Pisante, M. “Past and future of plant stress detection: an overview from remote sensing to positron emission tomography,” Frontiers in Plant Sci. 11: 609155 (2021).

[12] Zhang, Z., Boubin, J., Stewart, C., and Khanal, S. “Whole-field reinforcement learning: a fully autonomous aerial scouting method for precision agriculture,” Sensors 20: 6585 (2020).

[13] Cerro, J., Ulloa, C. C., Barrientos, A., and Rivas, J. de L. “Unmanned aerial vehicles in agriculture: a survey,” Agronomy 11: 203 (2021).

[14] Yang, G., Liu, J., Zhao, C., Li, Z., Huang, Y., Yu, H., Xu, B., Yang, X., Zhu, D., Zhang, X., Zhang, R., Feng, H., Zhao, X., Li, Z., Li, H., and Yang, H. “Unmanned aerial vehicle remote sensing for field-based crop phenotyping: current status and perspectives,” Front. Plant Sci. 8:1111 (2017).

[15] FloraPulse.com. Accessed on December 4, 2021.

[16] Dynamax.com. Accessed on December 4, 2021.

[17] Hossain, N. I., Noushin, T., Tabassum, S. **“**Leaf-FIT: a wearable leaf sensor for in-situ and real-time monitoring of plant phytohormones,” in the Proceedings of IEEE Sensors Conference*,* Oct 31- Nov 4 (2021). DOI: 10.1109/SENSORS47087.2021.9639842

[18] Srivastava, S. K., Arora, V., Sapra, S., and Gupta, B. D., “Localized surface plasmon resonance-based fiber optic U-shaped biosensor for the detection of blood glucose,” Plasmonics 7, 261-268 (2012).

[19] S. Wang, W. Deng, L. Yang, Y. Tan, Q. Xie, and S. Yao, “Copper-based metal-organic framework nanoparticles with peroxidase-like activity for sensitive colorimetric detection of staphylococcus aureus,” ACS Appl. Mater. Interfaces 29, 24440–24445 (2017).

[20] L. -J. Sun et. al. Electrochemical mapping of indole-3-acetic acid and salicylic acid in whole pea seedlings under normal conditions and salinity. *Sensors and Actuators B: Chemical*, 276: 545-551, 2018.

[21] Y. Hu, J. Zhao, H. Li, X. Wang, P. Hou, C. Wang, A. Li, and L. Chen. In vivo detection of salicylic acid in sunflower seedlings under salt stress. *RSC Adv.* 8: 23404, 2018.

[22] H. -R. Wag, X. -M. Bi, Z. -J. Fang, H. Yang, H. -Y. Gu, L. -J. Sun, and N. Bao. Real time sensing of salicylic acid in infected tomato leaves using carbon tape electrodes modified with handed pencil trace. *Sensors and Actuators B: Chemical* 286: 104-110, 2019.

[23] A multifunctional ratiometric electrochemical sensor for combined determination of indole-3- acetic acid and salicylic acid. *RSC Adv.* 10: 3115, 2020.

[24] A. H. Elhakem. Salicylic acid ameliorates salinity tolerance in maize by regulation of phytohormones and osmolytes. *Plant, Soil and Environment,* 66:533–541, 2020.

[25] A. A. H. A. Latef, A. Akter, and Md. T. Ul-Arif. Foliar application of auxin or cytokinin can confer salinity stress tolerance in Vicia faba L. *Agronomy* 11: 790, 2021.

[26] M. Sharma and A. Laxmi. Jasmonates: emerging players in controlling temperature stress tolerance. *Frontiers in Plant Sci.* 6:1129, 2015.

[27] G. Li, C. Zhang, G. Zhang, W. Fu, B. Feng, T. Chen, S. Peng, L. Tao, and G. Fu. Abscisic acid negatively modulates heat tolerance in rolled leaf rice by increasing leaf temperature and regulating energy homeostasis. *Rice* 13:18, 2020.

Downloaded From: https://www.spiedigitallibrary.org/conference-proceedings-of-spie on 03 Feb 2023
Terms of Use: https://www.spiedigitallibrary.org/terms-of-use